Vibration insensitive, interferometric measurements of mirror surface figures under cryogenic conditions.

James E. Millerd and Neal J. Brock
4D Technology Corporation 3280 E. Hemisphere Loop, Suite 112, Tucson, AZ 85706
james.millerd@4dtechnology.com

James W. Baer, Peter Spuhler
Ball Aerospace & Technologies Corp. PO Box 1062 Boulder, CO 80306

Keywords: interferometry, mirrors, figure testing, cryogenic

1. ABSTRACT

We report on a technique to measure the surface figure of mirrors under extreme vibrational conditions. Measurements are presented of the surface figure changes of Zerodur primary mirrors with both spherical and parabolic shapes, manufactured for the NASA Deep Impact program. Conditions ranged from room temperature to 130K. The interferometer was located outside the cryogenic vacuum chamber and did not require any active or passive vibration isolation. We show measurement repeatability of better than 1/500 waves RMS at 633nm.

2. BACKGROUND

Phase-stepping interferometry is an established method for measuring a variety of physical parameters ranging from the surface figure of mirrors to the displacement of solid objects.[1] Phase-shift interferometers typically have an element in the path of the reference wavefront that introduces three or more known phase steps or shifts. By detecting the intensity pattern with a detector at each of the phase shifts, the phase distribution of the object wavefront can be quantitatively calculated independent of any attenuation in either of the reference or object wavefronts. Both continuous phase gradients and discontinuous phase gradients (speckle waves) can be measured using this technique.

Temporal phase shifting using methods such as piezo-electric driven mirrors have been widely used to obtain high-quality measurements under otherwise static conditions. The measurement of transient or high-speed events requires either ultra high-speed temporal phase shifting (i.e., much faster than the event timescales), which is limited due to detector speed, or alternatively spatial phase shifting, which can acquire essentially instantaneous measurements.

Testing optics under cryogenic temperatures requires the use of a thermal vacuum chamber, which introduces large thermal gradients and is subject to significant vibrations due to the vacuum pumps and the long standoff distances necessary. The resulting environments are far more hostels than those in optical laboratories where mirrors can be tested on vibration-isolated equipment. It is possible to isolate the entire chamber from vibration,[2,3] or put vibration isolation within a vacuum chamber; however, test equipment must either be placed inside the vacuum, or positioned on a separate isolation system outside the chamber. Alternatively, active vibration cancellation systems can be used to phase-lock the interferometer to a single point in the interferogram.[4] All of these approaches have been demonstrated successfully, but they are difficult and often expensive to implement.

Spatial phase shifting overcomes problems due to vibration in the measurement path by recording all the necessary phase-stepped interferograms at the same time. Smythe and Moore described a spatial phase-shifting method in which a series of conventional beam splitters and polarization optics are used to produce three or four phase-shifted images onto as many cameras for simultaneous detection.[5] One of the disadvantages of this method is that multiple cameras are required and complicated optical arrangements are needed to produce the phase-shifted images, resulting in expensive and complex systems.

Other methods of spatial phase shifting include the use of gratings to introduce a relative phase step between the incident and diffracted beams. However, the grating must maintain sub-micron tolerances to accurately control the phase step between the beams. Spatial phase shifting has also been accomplished by using a tilted reference wave to induce a spatial carrier frequency to the pattern. This method requires the phase of the object field to vary slowly with respect to the detector pixels; therefore, steep slopes can present difficulties for this technique.

3. PHASECAM DESCRIPTION

The PhaseCam™ interferometer uses a form of spatial phase-shift interferometry to accomplish instantaneous phase-shift measurements.[6] Figure 1 shows the basic optical configuration, which employs a Twyman-Green interferometer, and generates simultaneous phase-shifted interferograms on a single sensor array. The optical system works by dividing orthogonally polarized reference and object beams into 4 identical copies that are then imaged contiguously onto a single CCD sensor array. A special holographic optical element is used to divide the interferograms. Each interferogram receives a different relative phase shift via a polarization quadrant mask that is placed on top of the detector array. The polarization mask consists of a combination of quarter waveplates and polarizers such that the four quadrants produce interferograms shifted by 90 degrees.

By using a single detector array instead of 4, the interferometer is compact and easy to align, is insensitive to motion of the detector array (because all pixels translate together), and has a simplified camera interface requirement. By using a fixed polarization mask instead of relying on a grating to provide a phase shift, there is greatly reduced sensitivity to the alignment of the holographic diffraction grating and calibration is maintained even in harsh operational environments. Finally, because both object and reference beams are common path through the holographic element, non-uniformities or imperfections do not produce errors in the measurement.

4. MEASUREMENT ERROR SOURCES

Although highly immune to vibration, spatial phase-step interferometers are susceptible to systematic errors which can limit system performance.[7] The errors sources can be categorized in two groups; those common to temporal and spatial phase-shifting interferometers and those unique to the spatial technique. Examples of common error sources are:

a) Optical component figuring. The surface quality of the beamsplitter, reference mirror and coupling (or diverging) optics will produce wavefront errors. Fortunately these errors can be measured, stored as a calibration surface, and subtracted from subsequent measurements to produce corrected surface measurements.
b) Quantization and shot noise. Random noise resulting from shot noise in the detector and quantization roundoff will produce errors in single measurements. Due to the random nature, averaging can be used to effectively reduce this noise.

The error sources unique to the PhaseCam technique are:

c) Pixel matching between interferograms. Registration of the 4 interferograms with respect to each other is critical to obtaining good instrument performance. In multi-camera implementations, there are 6 degrees of freedom with respect to the alignment of the detector plane and the interferogram (x, y, z, plus rotations about each of the three axes). Because all the detector pixels for the PhaseCam are located in the same plane, which can be accurately oriented normal to the optical axis, the degrees of freedom are effectively reduced to two, x and y. The x, y registration of the pattern can be accurately measured to sub-pixel accuracy by projecting a fiducial pattern through the system. The magnitude of the measurement error produced by a given pixel mis-match is relatively small at null or infinite fringe conditions but grows quickly with increased spatial frequency of the interference pattern (tilt or defocus). The spatial frequency dependence of the error can be used to identify its existence in the presence of other error sources.
d) Intensity balance between interferograms. Because each phase of the interference pattern is detected by separate pixels, losses in each channel and the individual gain and offset of each pixel will introduce phase dependent errors. Figure 2 illustrates the phase-dependent error caused by intensity imbalance between two quadrants of 10%. Fortunately, these losses are static, can be measured during initial calibration and corrected by scaling data at each pixel.
e) Alignment and accuracy of the polarization optics. Both the orientation and quality of the polarization optics can introduce a measurement error. Figure 2 also illustrates the phase-dependent error caused by a waveplate retardance error of 4 degrees. Clearly, even these small error sources can introduce significant measurement errors if left uncorrected. Once again, because the errors are static, they can be measured and compensated for;

however, the compensation must be done using a modified phase calculation algorithm rather than scaling the interferogram data.

5. CALIBRATION MEASUREMENTS

To gage the accuracy and repeatability of the PhaseCam interferometer under otherwise ideal conditions we performed a series of measurements of calibration surface, which was a two inch diameter, flat mirror having a reflectivity of 90%, and a surface figure <λ/20 PV at 633nm. The calibration surface was positioned close to the interferometer; air turbulence and vibrations were minimized. The interferograms were taken in ten groups of 16. Tilt was fit and removed from each individual measurement. From this series of measurements we calculate the following parameters:

a) **Calibrated Surface:** defined as the surface resulting from a pixel-by-pixel average of all surface measurements of calibration target.

$$CalibratedSurface(x,y) = \frac{1}{N}\sum_{i=1}^{N} Surface_i(x,y)\ ;\ \text{N=10;}$$

b) **Uncalibrated accuracy**: Statistical average of PV for each of the 10 surface measurements.

$$\frac{1}{N}\sum_{i=1}^{N} PV_i\ ;\ \text{N=10}$$

f) **RMS Repeatability:** 1 sigma (standard deviation) for the 10 measurements

$$\frac{1}{N}\sqrt{\sum_{i=1}^{N}\left(RMS_i - AveRMS\right)^2}\ ;\ \text{N=10}$$

g) **RMS Precision:** Average RMS of the difference between measured surface and the calibrated surface.

$$\frac{1}{N}\sum_{i=1}^{N} RMS\left(Surface_i(x,y) - CalibratedSurface(x,y)\right);\ \text{N=10}$$

Table 1 shows the calculated performance parameters for the PhaseCam with the calibration surface. The limiting factor in uncalibrated peak-to-valley accuracy was the polarizing beamsplitter surface quality.

Uncalibrated Accuracy (PV)	Repeatability (RMS)	Precision (RMS)
0.05 waves	0.0004 waves	0.0069 waves

6. CRYOGENIC MIRROR TESTING

NASA's Deep Impact mission to Comet Temple 1 will include 300 and 120 mm aperture reflective telescopes. The entire scientific imaging suite will be passively cooled by exposure to deep space and shielding from the sun. Thermal modeling predicts that the primary mirror will stabilize at 130 K. To achieve good imaging performance, it is critical that the mirrors maintain their optical figure at the nominal operational temperature; therefore, testing under cryogenic conditions is necessary.

Zerodur was selected for the mirror substrates based on its low CTE and the breadth of the temperature range over which this CTE remains low. A single lot of four mirror blanks were purchased from Schott, and light-weighted using CNC machining. To mount the mirror, small Invar pads will be bonded to its periphery. Structural analysis predicted that significant stress would be induced over the 170K differential from room temperature, even with the small difference in expansion between Zerodur (+0.001% expansion) and Invar (0.031% contraction). The initial plan was to observe this stress induced figure distortion of a mounted mirror and to correlate it to the FEM predictions. The goal was to confirm that the distortion would not consume a significant fraction of the system wavefront error budget of 70 nm RMS (λ/10 at 700 nm).

The Deep Impact mirrors were tested under ambient and cryogenic conditions as shown in Figure 3. The interferometer, as deployed outside the vacuum chamber, is shown in Figure 4. A real-time video frame of the four phase-shifted interferograms simultaneously imaged on a single CCD array is shown in Figure 5. The PhaseCam includes a fast CCD that can limit the exposure time to as little as 30 microseconds. This allows the system to record interferograms in a

manner insensitive to vibrations below about 10 kHz, and through turbulent air. Multiple interferograms were recorded and averaged similar to the calibration procedure.

7. SPHERICAL MIRROR TESTS

For the initial testing, an Engineering Model mirror was polished with a spherical surface, and held in a sling mount, facing a side port of the vacuum chamber. The port was sealed with a meniscus window. The PhaseCam head, with its diverging F/7 beam, was placed so that its source point was at the center of curvature of the mirror[1]. Interferograms were observed, although each one had up to several waves of random tilt due to the environmental vibration. This was not surprising considering the cantilevered platform on which the interferometer was mounted. Despite the challenging environment, the repeatability of the averaged wavefronts remained below 0.0006 waves RMS.

Measurements were recorded at each step of the test. This included an initial set-up before the window was installed. Additional measurements were recorded through the window, after the vacuum was established, and at various temperatures during the two day cool-down. Corresponding measurements were made as the mirror was warmed, and as the chamber was returned to room temperature and ambient pressure, and with the window removed. Figure 6 shows the calculated repeatability of the instrument as a function of mirror temperature. The numbers remain well below 0.001 waves RMS. Using fiducials placed on the mirror surface, the interferograms were precisely overlayed, and numerically subtracted. The room temperature measurements before and after cooling and heating differed by <<0.01 waves RMS.

During cooldown, a significant amount of distortion in the mirror was observed. The RMS surface figure error was recorded at several temperatures. These values are plotted in Figure 7. The thermo-mechanical distortion was best seen by taking the differences between the surface profile at a reduced temperature and at ambient temperature. This difference peaked at 0.075 waves RMS. A map of the differential figure is shown in Figure 9.

To discern whether this effect was inherent to the mirror or an artifact of the test, the mirror was rotated 120°, which matched its internal symmetry, and the test repeated. Figure 7 includes the RMS figure error measurements for both runs, where the second data set is distinguished as “Rotated”. The figure irregularity repeats quite precisely. When these irregularities were quantified as third order aberrations, their magnitudes and orientations were seen to remain the same, and to remain in the same physical relation to the mirror substrate. That is, the axes of the apparent coma and astigmatism rotated 120° with the mirror to a precision of ~5°.

8. PARABOLIC MIRROR TESTING

Testing of parabolic mirrors is more challenging than spherical mirrors because position errors that displace the source from the center of curvature of the parabolic mirror will generate coma and astigmatism. In addition, testing a parabola without null corrector optics results in spherical aberration of third and higher orders.

Despite the additional opto-mechanical sensitivity we obtained good data testing parabolic mirrors. The stability of the measurements can be quantified by comparing repeated measurements. While each displayed surface profile is the average of many individual interferograms, multiple profiles can be obtained in a short time. To quantify the repeatability, we plot in Figure 8 the standard deviation of the surface irregularity. With the exception of one case with higher than average irregularity, the repeatability values remain below 1/1000 of a wave RMS, or about 4% of the irregularity being measured.

9. MOUNTED MIRROR TESTING

The affect of mounting configuration on mirror figure was also tested. The mirror was suspended in the chamber by three flexures, each of which was attached to one of the Invar mounting pads, which were bonded to the mirror’s edge. The bulk distortion, as measured in the sling mounted tests, was subtracted using a point-by-point subtraction in software. Spherical aberration was removed using a software fitting routine. Figure 10 is a map of the remaining surface figure difference between ambient and operational temperature. The figure clearly shows expected distortion of the mirror surface in the immediate vicinity of the three mounting pads. The Peak-to-Valley range is 0.43 waves, with

much of this outside the clear aperture. By masking the three regions of distortion, it was possible to estimate the contribution to surface figure within the clear aperture to be 0.011 waves RMS.

10. CONCLUSION

Interferometric testing of optics in rugged environments can be readily conducted using the PhaseCam Interferometer. To obtain accurate and repeatable measurements it is necessary to carefully calibrate the instrument, however this only needs to be performed once. The PhaseCam was used to measure the figure of 300 mm diameter mirrors at cryogenic temperatures. The repeatability of the measurements was below 0.001 waves, despite the high vibration environment, only slightly worse than measurements made under ideal conditions. Testing of parabolic mirrors is more difficult than testing spheres, because displacements of the interferometer introduce aberrations, but this testing was also successful. This testing clearly measured the mounting induced distortion of 0.011 waves RMS magnitude.

11. ACKNOWLEDGEMENTS

This work was performed, in part, under the University of Maryland contract for the Deep Impact Instruments, in support of NASA's Deep Impact Discovery class mission being lead by the Jet Propulsion Laboratory in Pasadena, CA.

12. REFERENCES

1. Optical Shop Testing, 2nd ed Daniel. Malacara, editor, John Wiley & Sons, 1992
2. Cryogenic surface distortion and hysteresis of a 50 cm diameter fused silica mirror at 77 K" Jeffrey A. Young, et. al., "Cryogenic Optical Systems and Instruments IV" SPIE Vol. 1340 P 111 (1990)
3. The SIRTF Telescope Test Facility: The First Year, Melora Larson, et. al., "Cryogenic Optical Systems and Instruments VIII" SPIE Vol. 2814 P 2 (1996)
4. R. Smythe, R. Moore "Instantaneous phase measuring interferometry" *Optical Engr.* Vol. 23, No. 4, p. 361, 1984.
5. J. Hayes "Dynamic Interferometry Handles Vibration" Laser Focus World, p109, March 2002.
6. J. E. Millerd and N. J. Brock, US Patent No. 6,304,330 "*Methods and Apparatus for splitting imaging and measuring wavefronts in interferometry,*" Oct 16, 2001
7. A. Hettwer, J. Kranz, J. Schwider, "Three channel phase-shifting interferometer using polarization-optics and a diffraction grating," Optical Engineering, pp 960, Vol. 39 No. 4, April 2000.

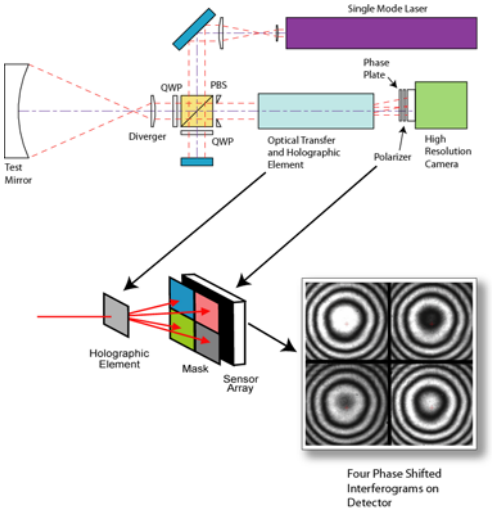

Figure 1 PhaseCam optical layout

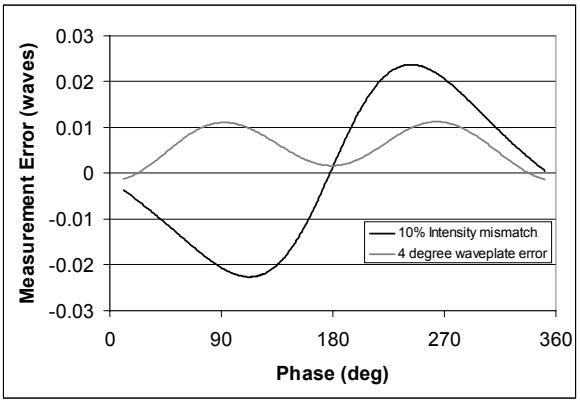

Figure 2. Effects of error sources on measurement linearity

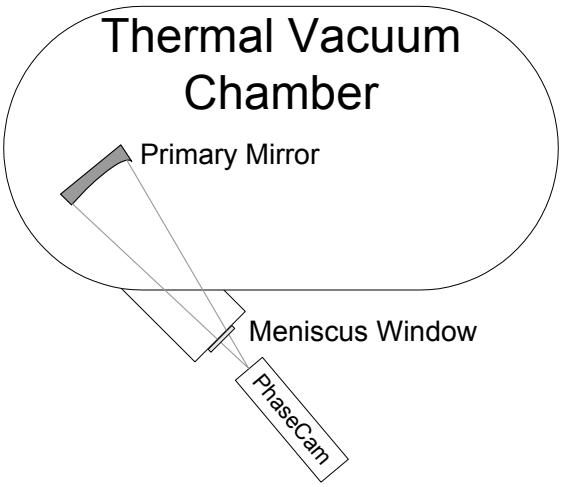

Figure 3 Testing configuration with the Thermal Vacuum Chamber

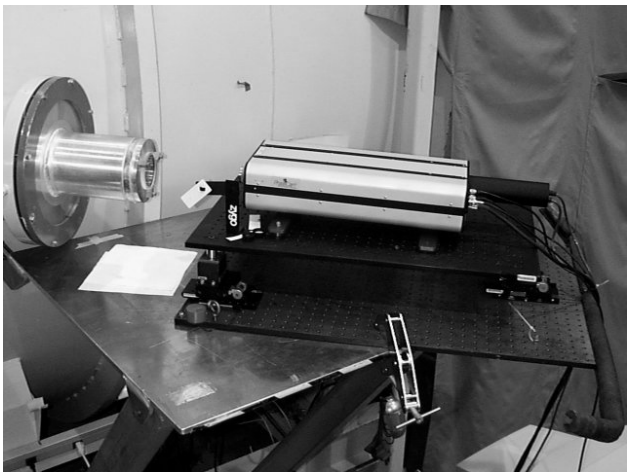

Figure 4 PhaseCam in Operation at the Thermal Vacuum Chamber

Figure 5 Real-time video display of four simultaneous interferograms

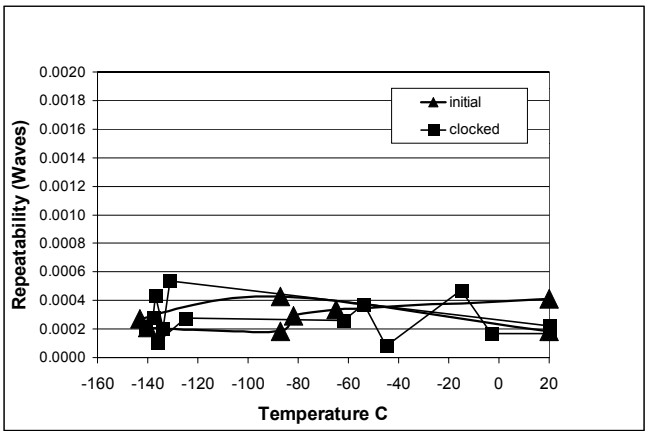

Figure 6 Spherical Mirror Figure Measurement Repeatability

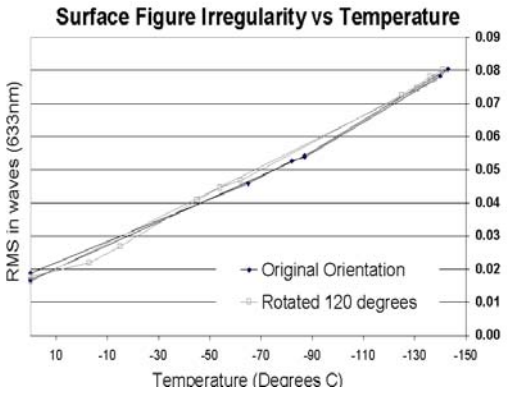

Figure 7 Spherical Mirror Irregularity vs Temperature

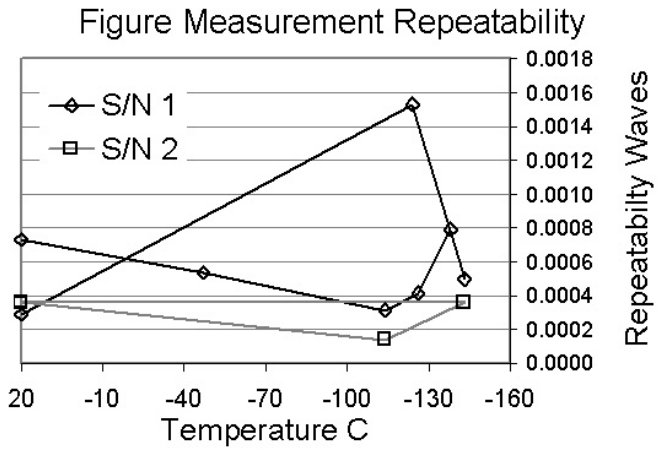

Figure 8 Parabolic Mirror Figure Measurement Repeatability

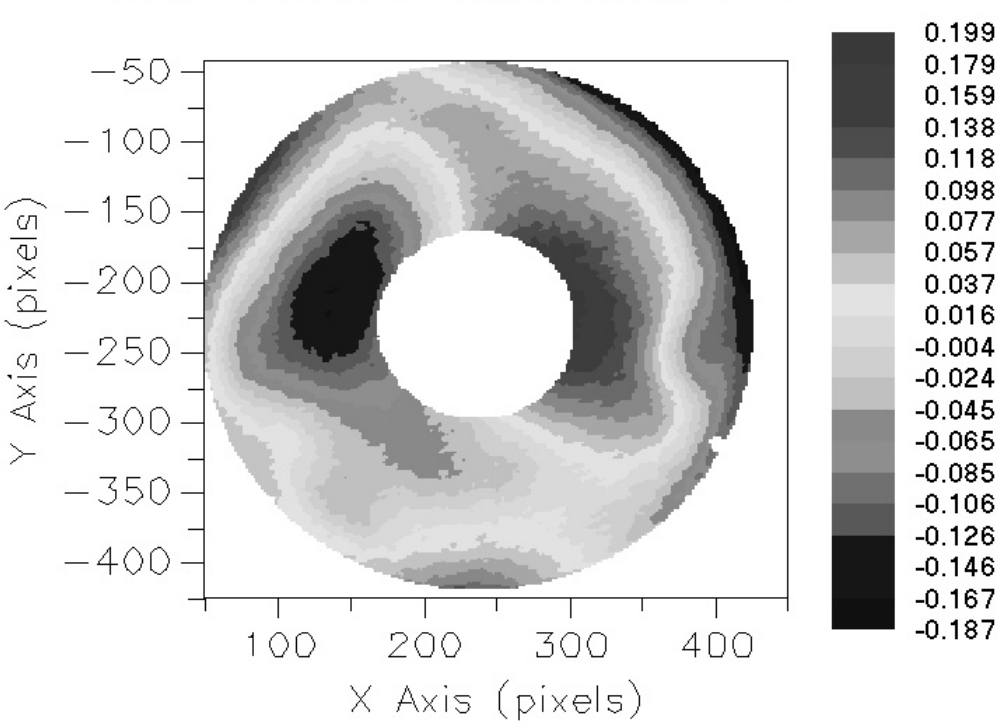

Range (PV) = 0.3863 waves, RMS = 0.0754 waves, Strehl = 0.7989
Analysis Aper: Pos[237, 231] Size[379, 379]

Figure 9 Spherical Mirror Differential Surface Figure between +20C and -141°C

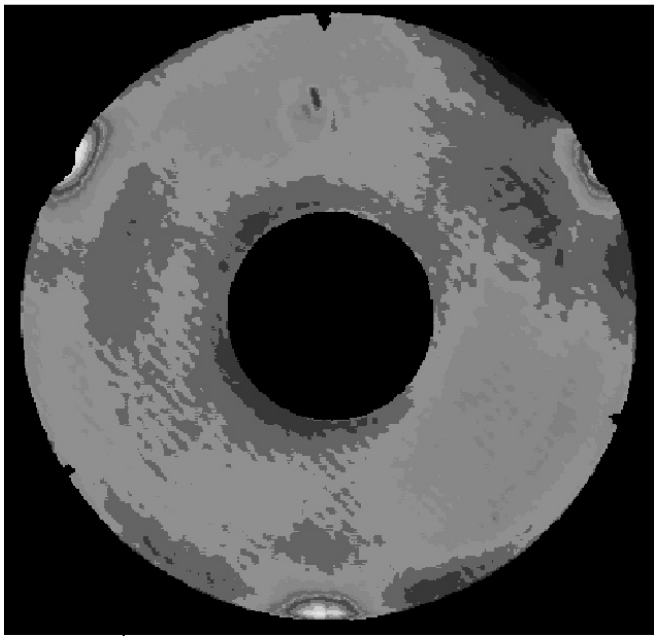

Figure 10 Pinching observed in the mounted parabolic mirror at –140 C